

# Frequency responses of age-structured populations: Pacific salmon as an example

Lee Worden<sup>a,b,\*</sup>, Louis W. Botsford<sup>c</sup>, Alan Hastings<sup>b</sup>, Matthew D. Holland<sup>c</sup>

<sup>a</sup>*Department of Biology, Theoretical Biology Lab, McMaster University, LS 332 1280 Main Street West, Hamilton, ON L8S 4K1 Canada*

<sup>b</sup>*Department of Environmental Science & Policy, University of California, Davis, One Shields Ave, Davis, California 95616 USA*

<sup>c</sup>*Department of Wildlife, Fish, & Conservation Biology, University of California, Davis, One Shields Ave, Davis, California 95616 USA*

---

## Abstract

Increasing evidence of the effects of changing climate on physical ocean conditions and long-term changes in fish populations adds to the need to understand the effects of stochastic forcing on marine populations. Cohort resonance is of particular interest because it involves selective sensitivity to specific time scales of environmental variability, including that of mean age of reproduction, and, more importantly, very low frequencies (i.e., trends). We present an age-structured model for two Pacific salmon species with environmental variability in survival rate and in individual growth rate, hence spawning age distribution. We use computed frequency response curves and analysis of the linearized dynamics to obtain two main results. First, the frequency response of the population is affected by the life history stage at which variability affects the population; varying growth rate tends to excite periodic resonance in age structure, while varying survival tends to excite low-frequency fluctuation with more effect on total population size. Second, decreasing adult survival strengthens the cohort resonance effect at all frequencies, a finding that addresses the question of how fishing and climate change will interact.

---

\*Corresponding author

*Email addresses:* worden.lee@gmail.com (Lee Worden), lbotsford@ucdavis.edu (Louis W. Botsford), amhastings@ucdavis.edu (Alan Hastings), mdholland@ucdavis.edu (Matthew D. Holland)

1 **1. Introduction**

2 In population theory, interest is increasing in the complex ways in which  
3 age-structured, density-dependent populations respond selectively to different  
4 time scales (or frequencies) of variability in the environment. These questions  
5 dovetail with the increasing practical need to understand how populations will  
6 respond to potential changes in life history parameters and the time scales of en-  
7 vironmental variability due to climate change and increasing pressure on natural  
8 resources such as fisheries. There is a growing awareness that model population  
9 responses can appear to filter certain frequencies in environmental variability  
10 (Greenman and Benton, 2005). Furthermore, these effects can serve to amplify  
11 variability by exciting modes of population behavior that without environmental  
12 variability would be locally stable (Greenman and Benton, 2003). One exam-  
13 ple of such behavior, cohort resonance, is closely identified with life history  
14 characteristics in that it features cycles of period equal to the dominant age of  
15 reproduction. (Bjørnstad et al., 1999).

16 There is particular interest in the dynamic responses of the marine fish tar-  
17 getted by global fisheries as they are subject to a dramatic artificial change in a  
18 life history parameter, adult survival, and there are indications that the domi-  
19 nant time scales of environmental variables such as ENSO that affect fish popula-  
20 tions may change with a changing climate (Timmermann et al., 1999). Empiri-  
21 cal observations and models indicate that variability in fish populations increases  
22 with increased fishing (Hsieh et al., 2006; Anderson et al., 2008). The cohort  
23 resonance phenomenon in fish populations presents particular problems for cli-  
24 mate change because it enhances sensitivity to very slow signals (trends) in ad-  
25 dition to those at the period of dominant age of reproduction (Bjørnstad et al.,  
26 2004). Observations of such effects could be confounded with potential slow  
27 changes in the environment, and thus make it difficult to differentiate between  
28 them.

29        Within the general concern for the combined effects of fishing and climate  
30 change on marine ecosystems (Perry et al., 2010), there is a particular interest  
31 in the effects of the marine environment and fishing on population dynamics of  
32 Pacific salmon on annual to decadal time scales. Analyses of the influences of the  
33 ocean environment on Pacific salmon, whether statistical examination of covari-  
34 ability between population and environmental variables (*e.g.*, Logerwell et al.,  
35 2003) or estimation of survivals to specific sizes and ages through analysis of  
36 coded wire tagging data (*e.g.*, Coronado and Hilborn, 1998; Teo et al., 2009),  
37 commonly assume the variable ocean environment influences survival during  
38 the early ocean phase of this anadromous genus. In fewer cases environmental  
39 variability in the age of maturation has been the dependent population variable  
40 (*e.g.*, Pyper et al., 1999).

41        These empirical findings raise questions regarding the relative roles of ran-  
42 dom variability in survival at various ages, and in the age distribution of repro-  
43 duction, in salmon population dynamics. Random survival is typically assumed  
44 to influence abundance directly, but the effects of varying age of spawning are  
45 not as clear, and there is a need to understand differences in population response  
46 to these two sources of random variability.

47        Here we examine and compare the effects of environmental variability in  
48 survival and age of spawning on the magnitude and time scales of population  
49 variability. We are engaged in a study of the influence of the oceanographic  
50 environment on Pacific salmon, the GLOBEC North East Pacific program,  
51 part of the US Climate Change program. Earlier retrospective analyses in-  
52 dicated differences in the responses of the two California Current congeners,  
53 chinook salmon, *Oncorhynchus tshawytscha*, and coho salmon, *O. kisutch*, and  
54 hence we are interested in the population dynamic differences between them  
55 (Botsford and Lawrence, 2002). For instance, coho salmon collapsed synchronously  
56 along the coast between 1980 and 2000, and coho appear to have more high fre-  
57 quency variability than chinook in their catch record. These species differ in  
58 their age distribution of spawning and in other ways (Botsford et al., 2005). We  
59 have explored some of the differences in probabilities of extinction of populations

60 with these spawning age distributions in response to time-varying marine sur-  
61 vival (Hill et al., 2003; Botsford et al., 2005). In salmon, differences in maturity  
62 schedule are due to differences in size distribution (and therefore prior growth  
63 rate) (Young, 1999; Vollestad et al., 2004). Similar effects occur in other non-  
64 salmonid species (Day and Rowe, 2002). To avoid confusion, we note that the  
65 mechanisms studied here are neither (1) the indirect effect on survival of varying  
66 development rate due to consequent variation in time spent at higher mortality  
67 (*e.g.*, Moloney et al., 1994), nor (2) the interaction between age structure and  
68 over-compensatory density-dependent recruitment that causes cycles of period  
69 roughly twice the generation time (Ricker, 1954; Botsford, 1997).

70 In the models used here oscillations with period  $2T$  do not arise (where  $T$  is  
71 generation time or age of dominant effect on recruitment), primarily because of  
72 the form of stock-recruitment function we use, but the cyclic mode with period  
73  $T$  turns out to play a central role in our investigation. Recently Myers et al.  
74 (1998) explored stochastic forcing of a cyclic mode of variability of period  $T$  as  
75 a potential cause of observed cycles in sockeye salmon (*Oncorhynchus nerka*) in  
76 British Columbia, Canada. This mode is similar to the “echo effect” associated  
77 with linear age-structured models of semelparous species (Sykes, 1969). Myers et  
78 al. noted that while this mode would not be the dominant mode, it could appear  
79 clearly in solutions obtained through forcing by randomly varying survival. This  
80 was essentially cohort resonance, though they did not use that term.

81 The time scales (or frequency content) of the population response also de-  
82 pend on the mode of observation, *e.g.*, whether the data in a time series are  
83 recruitment, abundance or catch (Botsford, 1986; Anderson et al., 2008). The  
84 nature of a catch time series depends on fishing mortality rate, with higher fish-  
85 ing rates leading to higher frequencies of variability (Botsford, 1986; Hsieh et al.,  
86 2006). Differences between the spectra of recruitment and abundance have been  
87 illustrated by Bjørnstad et al. (2004) for Atlantic cod (*Gadus morhua*). The  
88 most commonly available measurement of salmon populations is annual catch,  
89 either in numbers or biomass, and occasionally the age distribution of catch  
90 is determined. Frequently catch can be assumed to be individuals who if not

91 caught would be spawning that year because they are near the mouth of (or in)  
92 the spawning river. In some streams, spawning escapement is also estimated,  
93 and sometimes the age composition of spawners is also estimated. Catch and  
94 escapement can be summed to obtain the total abundance of potential spawners  
95 in a year. Total population abundance at time  $t$  cannot be observed directly,  
96 but estimates can be obtained through cohort reconstruction from several years  
97 of age-specific data from catch and escapement.

98 Here we explore several aspects of the spectral response of marine fish popu-  
99 lation dynamics, using parameter values representative of two species of Pacific  
100 salmon over a range of survivals as examples. Our practical interests are in  
101 the combined effects of fishing and climate change, so we focus on effects of  
102 long-term changes in survival on the population response to various time scales  
103 of environmental variability. Note, however, that long-term declines in survival  
104 can also be caused by the climate, independent of the fishery, as occurred in  
105 California Current coho salmon between 1980 and 2000 (Botsford et al., 2005).  
106 We also explore the differences in responses to environmental forcing at differ-  
107 ent points in the life history (i.e. development rate vs. survival), and spectral  
108 differences between various kinds of observations (e.g., observations of recruit-  
109 ment vs. observations of total abundance). We present results in terms of the  
110 changing spectral responses, and relate the spectral response to the eigenvectors  
111 and eigenspace structure of the linearized model.

## 112 **2. Model Formulation**

113 To investigate these questions, we introduce a density-dependent, stochastic  
114 age-structured model which we can use to compare the effects of temporal vari-  
115 ability in the timing of reproduction and annual survivorship of salmon. Let  $n$   
116 be the maximum spawning age in years, and let  $\vec{x}(t) = (x_1(t), \dots, x_n(t))^T$  be

117 the age-structured population vector at year  $t$ . Then our model is

$$\vec{x}(t) = F(\vec{x}(t-1), t) = \begin{pmatrix} R(P(t)) \\ s(t) x_1(t-1) \\ s(t) x_2(t-1) \\ \vdots \\ s(t) x_{n-3}(t-1) \\ (1 - \delta_e(t)) s(t) x_{n-2}(t-1) \\ \delta_l(t) s(t) x_{n-1}(t-1) \end{pmatrix} \quad (1)$$

118 where  $P(t) = (\delta_e(t) x_{n-2}(t-1) + (1 - \delta_l(t)) x_{n-1}(t-1) + x_n(t-1))$  is the number  
 119 of fish returning to spawn in year  $t$ , and

$$R(P(t)) = \frac{\alpha P(t)}{1 + \beta P(t)} \quad (2)$$

120 is a Beverton-Holt density dependent recruitment term (Beverton and Holt,  
 121 1957). Thus the recruitment  $R(P(t))$  represents the number of outmigrants  
 122 (smolts) leaving a spawning stream in year  $t$ , resulting from egg production by  
 123 individuals of various spawning ages. We have assumed that migration from  
 124 freshwater to the marine environment occurs in the first year, and that there  
 125 is no difference in fecundity between the different ages of spawning. Parame-  
 126 ters  $\alpha$  and  $\beta$  characterize the density-dependent reproductive phase:  $\alpha$  is the  
 127 density-independent per-capita growth rate when the population is very small,  
 128 and  $\frac{\alpha}{\beta}$  is the maximum total number of offspring in the population. Timing  
 129 of reproduction is controlled by the remaining two parameters,  $\delta_e(t)$  and  $\delta_l(t)$ :  
 130 most individuals spawn at age  $n - 1$ ; a proportion  $\delta_e(t)$  of those surviving to age  
 131  $n - 2$  spawn at that age in year  $t - 1$ ; and a proportion  $\delta_l(t)$  of age  $n - 1$  fish in  
 132 year  $t$  postpone spawning until year  $t + 1$ , when they are age  $n$ . Annual survival  
 133  $s(t)$ , as written here, affects all age classes in year  $t$ . However, we also explore  
 134 the possibility that the dominant variability in ocean survival occurs during the  
 135 period immediately following ocean entry. This is a challenging stage for juve-  
 136 nile salmon, as they are completing the transition from freshwater to the marine  
 137 environment, and they are dependent on the highly variable food production in  
 138 the coastal ocean.

139 We are interested in understanding the time scales of variation in the solu-  
140 tions to the model (equation 1) in response to fluctuations in annual survivorship  
141 and timing of spawning. We do this by studying three cases: the case of fluctuat-  
142 ing survival  $s(t)$  at all ages, the case in which survival varies but only at the age  
143 of entry into the ocean, and the case in which fluctuating mean age of spawning  
144  $a(t)$  produces yearly changes in  $\delta_e(t)$  and  $\delta_l(t)$ . In all cases, the environmental  
145 fluctuation is a Gaussian white-noise signal,  $\xi(t) \in \mathbb{R}$  with  $E(\xi(t)) = 0$ . To  
146 model fluctuating survival we use  $s(t) = s^\circ + \xi(t)$ , where  $s^\circ$  is the unperturbed,  
147 constant survival. In the simulation the distribution of  $s(t)$  is truncated to en-  
148 sure that  $0 \leq s(t) \leq 1$ . To model fluctuating age of spawning, we suppose that  
149 individuals' ages of spawning are chosen from a normal distribution whose mean  
150 is the central age of spawning  $a(t)$  in year  $t$  (Fig. 1), specifically

$$p(a - a(t)) = \frac{1}{\sqrt{2\pi}\sigma} e^{-\left(\frac{a-a(t)}{\sqrt{2}\sigma}\right)^2}. \quad (3)$$

151 We approximate early and late spawning by having all early spawners spawn at  
152 age  $n - 2$  and all late spawners spawn at age  $n$ , so that

$$\delta_e(t) = \int_{-\infty}^{n-1.5} p(a - a(t)) da \quad (4)$$

153 and

$$\delta_l(t) = \int_{n-0.5}^{\infty} p(a - a(t-1)) da. \quad (5)$$

154 From the point of view of a cohort, the portions of that cohort that will spawn  
155 early and late, *i.e.*,  $\delta_e$  and  $\delta_l$ , are set by the value of  $a(t)$  in the year that that  
156 cohort transitions from age  $n - 2$  to age  $n - 1$ . That is,  $\delta_e(t)$  is a function of the  
157 central spawning age in year  $t$ , whereas  $\delta_l(t)$ , which has its effect a year after it  
158 is determined, is a function of the central spawning age in year  $t - 1$ . We model  
159 the fluctuating central age of spawning as  $a(t) = a^\circ + \xi(t)$ .

160 To compare the dynamics of the two salmon species along the west coast of  
161 the contiguous U.S., we have used parameter values that approximate known  
162 or likely values for the populations of coho and chinook salmon. Survival  
163 rates in the ocean are reasonably well known, and we consider three cases:  
164 a “typical” value of  $0.85 \text{ yr}^{-1}$  (Bradford, 1995), a “small” value of  $0.28 \text{ yr}^{-1}$ ,

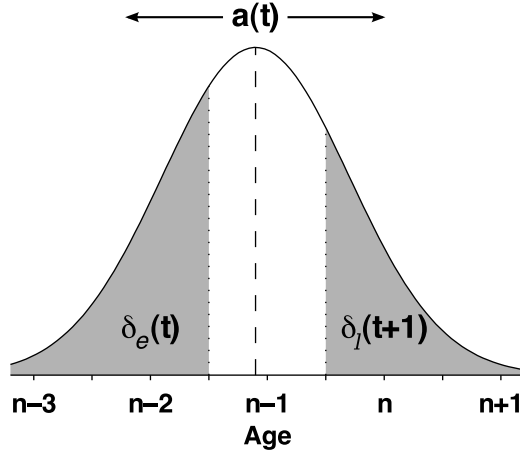


Figure 1: An example illustrating how the fraction of early and late spawners is modeled. The central spawning age  $a(t)$  varies from year to year. Here we picture a normal distribution of potential spawning age with mean  $a(t) = n - 1.1$  and  $\sigma = 0.8$ . The parameters representing the proportions of early spawners ( $\delta_e$ ) in year  $t$  and late spawners ( $\delta_l$ ) in year  $t + 1$  are the integrals of this function over  $(-\infty, n - 1.5]$  and  $[n - 0.5, \infty)$ , respectively.

165 and a “very small” value of  $0.2 \text{ yr}^{-1}$ , estimated from more recent observa-  
 166 tions of coho salmon. Since the “very small” value is not sustainable in the  
 167 chinook model, that case is not considered. The distributions of values of  $\alpha$   
 168 and  $\beta$  (equation 2) have been estimated for coho salmon, but not for chinook  
 169 salmon (Barrowman et al., 2003), and we use the modes from those distribu-  
 170 tions ( $\alpha = 60$  and  $\beta = 0.00017$ ). In chinook salmon populations in the California  
 171 Current, individuals typically spawn primarily at a single dominant age, with  
 172 less spawning at adjacent ages. The dominant age of spawning increases with  
 173 latitude (Hill et al., 2003). Here we chose dominant spawning at age 4, i.e.,  
 174  $n = 5$  and  $a^\circ = 4$ . Precocious spawning in chinook salmon ranges from 0–  
 175 10 percent in males and from 0–3 percent in females (Healey, 1991). We use  
 176  $\sigma = 0.4$ , which makes  $\delta_e = \delta_l \approx 0.1$ . Coho salmon in the California Current  
 177 spawn predominantly at age 3 with substantial precocious spawning at age 2  
 178 and minimal spawning at age 4. Precocious spawning in coho salmon consists  
 179 almost completely of males, is more variable than in chinook salmon, and can be  
 180 as high as 30 percent in natural wild populations (Sandercock, 1991). It is not

181 possible to observe the effects of precocious spawning by males on reproduction  
182 directly, but for coho salmon, a modification of genetic methods for estimating  
183 effective population size indicated the effective proportion of 2-year-olds to be  
184 35 percent in two naturally spawning populations (Doornik et al., 2002). For  
185 coho salmon we chose  $n = 4$ ,  $a^\circ = 2.75$  and  $\sigma = 0.2$ , which makes  $\delta_e \approx 0.1$  and  
186  $\delta_l \approx 0.0001$ . The standard deviation of the stochastic variation,  $\sigma_E$ , is 0.085 for  
variation in survival, and 0.2 for variation in mean spawning age.

Table 1: Model parameters and unperturbed values.

Parameter	Description	Coho Value	Chinook Value
$s^\circ$	annual survival rate, all ages	0.85, 0.28, 0.2	0.85, 0.28
$\delta_e$	proportion of age $n-2$ fish spawning	0.1056	0.1056
$\delta_l$	proportion of age $n-1$ fish delaying spawning to age $n$	$8.84 \times 10^{-5}$	0.1056
$\alpha$	slope at origin of Beverton-Holt stock-recruitment curve	60	60
$\beta$	saturation parameter of Beverton-Holt stock-recruitment curve	$1.7 \times 10^{-4}$	$1.7 \times 10^{-4}$
$a^\circ$	central age of spawning	2.75	4
$\sigma$	standard deviation of spawning age distribution	0.2	0.4
$\sigma_E$	standard deviation of environmental forcing signal	0.085 (survival) 0.2 (spawning age)	0.085 (survival) 0.2 (spawning age)

187

### 188 3. Model Analysis

189 In each of the model cases, the age vector  $\vec{x}$  converges to a neighborhood of a  
190 single point, and fluctuates in that neighborhood in response to the fluctuating  
191 life-history parameters. To find the center point, we consider the deterministic  
192 system defined by equation 1 with  $s$ ,  $\delta_e$ , and  $\delta_l$  all fixed at their unperturbed  
193 values. This system has a unique positive fixed point that is globally attracting

194 for positive trajectories:

$$\tilde{\vec{x}} = \begin{pmatrix} 1 \\ s \\ s^2 \\ \vdots \\ s^{n-3} \\ (1 - \delta_e)s^{n-2} \\ (1 - \delta_e)\delta_l s^{n-1} \end{pmatrix} \frac{\alpha - c}{\beta}, \quad (6)$$

195 where  $1/c = \delta_e s^{n-3} + (1 - \delta_e)(1 - \delta_l)s^{n-2} + (1 - \delta_e)\delta_l s^{n-1}$  is the amount of  
 196 spawning in the lifetime of the average smolt.

197 As we will see, we can understand a great deal about the population dynam-  
 198 ics by looking at the linearized dynamics at this fixed point of the deterministic  
 199 dynamics. We linearize the effect of the stochastic noise term  $\xi(t)$  as well as the  
 200 age-structured population vector  $\vec{x}(t)$ :

$$\vec{y}(t) \approx \mathbf{J}\vec{y}(t-1) + \sum_{l=0}^L \vec{H}(l)\xi(t-l), \quad (7)$$

201 where  $\vec{y}(t) = \vec{x}(t) - \tilde{\vec{x}}(t)$  is the deviation from the fixed point,  $\mathbf{J}$  is the Jacobian  
 202 matrix of the dynamics at the fixed point, and linearizing in the noise term gives  
 203 a sequence of “forcing vectors”  $\vec{H}$  that summarizes how the noise enters into  
 204 the dynamics with various time lags (see the Appendix for details).

205 At the fixed point, the Jacobian matrix is

$$\mathbf{J} = \begin{pmatrix} 0 & \dots & 0 & \delta_e \frac{c^2}{\alpha} & (1 - \delta_l) \frac{c^2}{\alpha} & \frac{c^2}{\alpha} \\ s & & & & & 0 \\ & \ddots & & & & \vdots \\ & & s & & & \vdots \\ & & & (1 - \delta_e)s & & \vdots \\ & & & & \delta_l s & 0 \end{pmatrix}, \quad (8)$$

206 where all entries left blank are zero.

207 A linear system like this one decomposes naturally into independent subsys-  
 208 tems located in linearly independent one- and two-dimensional subspaces, each  
 209 characterized by a real eigenvalue or a complex pair of eigenvalues (Hirsch and Smale,  
 210 1974). The right eigenvectors of the Jacobian matrix are the basis vectors for  
 211 each of these subspaces of the dynamics. The complex conjugate eigenvalues  
 212 of the Jacobian predict the resonant frequencies of the population's response to  
 213 noise. In the time-varying-survival cases, we only need a single forcing vector  
 214  $\vec{H}$ , because the state of the environment in year  $t$ ,  $\xi(t)$ , only affects survival in  
 215 year  $t$ ; but in the varying-age-structure case, because conditions in year  $t$  affect  
 216 the number of early returns  $\delta_e$  in year  $t$  and the number of late returns  $\delta_l$  in  
 217 year  $t + 1$ , we have to include two forcing vectors to describe the effects with  
 218 and without one year's time lag.

219 In the case of fluctuating survival at all ages, the forcing is captured by the  
 220 vector  $\vec{H}_s(0)$ , with

$$\vec{H}_s(0) = \left( \frac{\partial F_i}{\partial \xi(t)} \right) = \begin{pmatrix} 0 \\ \tilde{x}_1 \\ \tilde{x}_2 \\ \tilde{x}_3 \\ \vdots \\ \tilde{x}_{n-3} \\ (1 - \delta_e)\tilde{x}_{n-2} \\ \delta_l\tilde{x}_{n-1} \end{pmatrix} = \begin{pmatrix} 0 \\ 1 \\ s^\circ \\ (s^\circ)^2 \\ \vdots \\ (s^\circ)^{n-4} \\ (1 - \delta_e)(s^\circ)^{n-3} \\ (1 - \delta_e)\delta_l(s^\circ)^{n-2} \end{pmatrix} \frac{\alpha - c}{\beta}. \quad (9)$$

221 We note that when survival is forced additively, as we have done here, the  
 222 deterministic system described above is not exactly the mean of the stochastic  
 223 system. A stochastic system with  $s(t) = s^\circ e^{\xi(t)}$  would have the deterministic  
 224 system as its mean, but in the limit of small noise, these representations have  
 225 identically-shaped frequency responses that merely differ by a factor of  $s$ . We  
 226 chose additive noise for convenience.

227 For forcing of survival at ocean entry, only survival to age 2 is subject to

228 fluctuation, so that

$$\vec{H}_{s_e}(0) = \begin{pmatrix} 0 \\ \frac{\alpha-c}{\beta} \\ 0 \\ \vdots \\ 0 \end{pmatrix}. \quad (10)$$

229 For time-varying ages of maturation, we have lag 0 effects from early spawn-  
230 ing

$$\vec{H}_a(0) = \left( \frac{\partial F_i}{\partial \xi(t)} \right) = \left( \frac{\partial F_i}{\partial \delta_e} \frac{\partial \delta_e}{\partial \xi(t)} \right) \quad (11)$$

231 and lag 1 effects from late spawning

$$\vec{H}_a(1) = \left( \frac{\partial F_i}{\partial \xi(t-1)} \right) = \left( \frac{\partial F}{\partial \delta_l} \frac{\partial \delta_l}{\partial \xi(t-1)} \right). \quad (12)$$

232 Since  $\frac{\partial a(t)}{\partial \xi(t)} = 1$  we have

$$\frac{\partial \delta_e(t)}{\partial \xi(t)} = \int_{-\infty}^{n-1.5} -p'(a-a(t)) da = -p(n-1.5-a(t)) \quad (13)$$

233 and

$$\frac{\partial \delta_l(t)}{\partial \xi(t-1)} = \int_{n-0.5}^{\infty} -p'(a-a(t-1)) da = p(n-0.5-a(t-1)). \quad (14)$$

234 The vector derivatives we need are

$$\left( \frac{\partial F_i}{\partial \delta_e} \right) = \begin{pmatrix} s^{n-3} \frac{c^2}{\alpha} \\ 0 \\ \vdots \\ 0 \\ -s^{n-2} \\ 0 \end{pmatrix} \frac{\alpha-c}{\beta} \quad (15)$$

235 and

$$\left( \frac{\partial F_i}{\partial \delta_l} \right) = \begin{pmatrix} -(1-\delta_e^\circ) s^{n-2} \frac{c^2}{\alpha} \\ 0 \\ \vdots \\ 0 \\ (1-\delta_e^\circ) s^{n-1} \end{pmatrix} \frac{\alpha-c}{\beta}, \quad (16)$$

236 where  $\delta_e^\circ$  refers to the unperturbed value of  $\delta_e$ . Substituting (13) and (15) into  
 237 (11) yields the forcing at lag 0,

$$\vec{H}_a(0) = \begin{pmatrix} -p(n - 1.5 - a^\circ)s^{n-3}\frac{c^2}{\alpha} \\ 0 \\ \vdots \\ 0 \\ p(n - 1.5 - a^\circ)s^{n-2} \\ 0 \end{pmatrix} \frac{\alpha - c}{\beta}. \quad (17)$$

238 Substituting (14) and (16) into (12) gives the forcing at lag 1,

$$\vec{H}_a(1) = \begin{pmatrix} -p(n - 0.5 - a^\circ)(1 - \delta_e^\circ)s^{n-2}\frac{c^2}{\alpha} \\ 0 \\ \vdots \\ 0 \\ p(n - 0.5 - a^\circ)(1 - \delta_e^\circ)s^{n-1} \end{pmatrix} \frac{\alpha - c}{\beta}. \quad (18)$$

## 239 4. Results

### 240 4.1. Dynamics near the fixed point

241 Each of these models without random fluctuation has a unique positive fixed  
 242 point (equation (6)). The condition for a fixed point can be illustrated in terms  
 243 of the stock-recruitment function and a straight line through the origin with  
 244 slope equal to the inverse of mean lifetime egg production, as shown in Fig. 2  
 245 (Sissenwine and Shepherd, 1987). The fixed point lies at the intersection of  
 246 these, allowing clear interpretation of the effects of long-term changes in sur-  
 247 vival. As mean ocean survival declines, equilibrium egg production declines,  
 248 and eventually recruitment declines. For the very low survival rate for chinook  
 249 salmon, the fixed point is zero indicating survival is not adequate for persis-  
 250 tence. Because the parameters for the stock-recruitment relationship and the  
 251 estimated survivals are for coho salmon, this has no implications for real chinook  
 252 salmon populations.

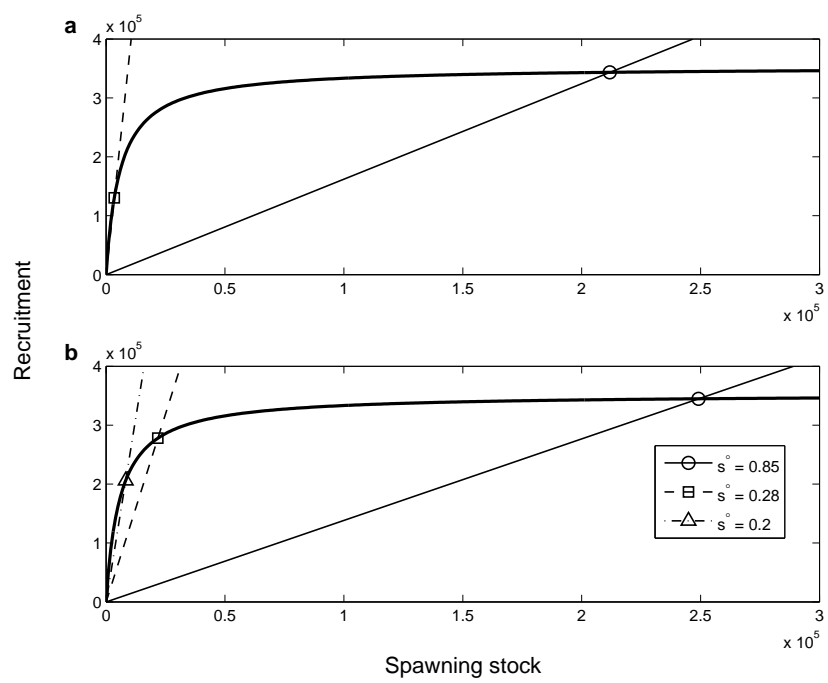


Figure 2: Graphical interpretation of the equilibrium recruitment as the intersection of the smolt-adult curve and a line through the origin with slope  $1/(\text{lifetime reproduction})$  for (a) chinook and (b) coho salmon.

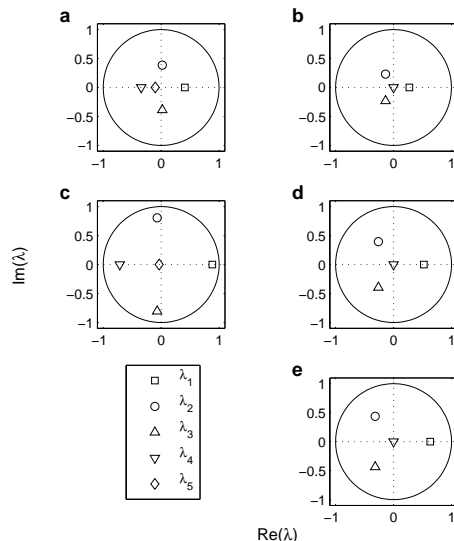


Figure 3: Eigenvalues of linearization matrix  $\mathbf{J}$  in chinook and coho models for typical survival: (a) chinook,  $s = 0.85 \text{ yr}^{-1}$ , (b) coho,  $s = 0.85 \text{ yr}^{-1}$ ; small survival: (c) chinook,  $s = 0.28 \text{ yr}^{-1}$ , (d) coho,  $s = 0.28 \text{ yr}^{-1}$ ; and very small survival: (e) coho,  $s = 0.2 \text{ yr}^{-1}$ .

253 Plots of the eigenvalues of the linearization at the fixed point of each of  
 254 these models indicate the modes of variability, and how they change with sur-  
 255 vival (Figure 3). Note that the chinook model has 5 eigenvalues, while the coho  
 256 model has 4 eigenvalues because those are the maximum ages in each model  
 257 population. In both the chinook and coho models, the linearized population  
 258 dynamics respond most strongly to forcing in the one-dimensional mode corre-  
 259 sponding to the positive real eigenvalue,  $\lambda_1$  (the dominant mode of variability).  
 260 Motion in this mode occurs without oscillation, that is, at low frequencies. The  
 261 next strongest mode is a resonance at period  $n - 1$  or a little less (determined by  
 262 the eigenvalues  $\lambda_2$  and  $\lambda_3$ , whose angle from the positive axis is approximately  
 263  $\pm \frac{2\pi}{n-1}$ ), indicating oscillations with a period equal to one generation time. In the  
 264 chinook case (Figures 3a,c) there is also a strong resonance at period two, corre-  
 265 sponding to a negative eigenvalue, and in all cases there is a weakly resonating  
 266 negative eigenvalue as well.

267 In both the chinook and the coho cases, the effect of decreasing the mean  
 268 survival is to move all eigenvalues outward toward the unit circle, increasing the

269 return time of all subsystems of interest and thereby increasing the expected  
270 magnitude of the cumulative response to variation over time. This effect is  
271 especially strong in the chinook model for “small”  $s$  (Fig. 3c). This occurs  
272 because the rate of change of recruitment with adult stock increases substantially  
273 as the survival declines (Fig. 2). Therefore, low equilibrium abundances in  
274 Figure 2 correspond to large magnitude eigenvalues (and, thus, large responses  
275 to variation) in Figure 3.

276 The spread in ages of spawning has a relatively small specific influence on  
277 the locations of the eigenvalues. When  $\sigma = 0$ , all fish spawn at age  $n - 1$ ,  
278 and the eigenvalues are roots of a simple characteristic polynomial,  $P(\lambda) =$   
279  $\lambda(\lambda^{n-1} - s^{n-2} \frac{c^2}{\alpha})$ . There is one zero root and the others are equal in size  
280 and evenly spaced around zero (not shown). As  $\sigma$  increases, the dominant,  
281 positive real eigenvalue moves outward on the negative real axis, the others  
282 move inward slightly and the complex eigenvalues rotate slightly, their polar  
283 angles becoming slightly smaller in the chinook case and slightly larger in the  
284 coho case. In all cases other than  $\sigma = 0$ , the positive eigenvalue is largest in  
285 magnitude (consistent with the Perron-Frobenius theorem, since the entries of  $\mathbf{J}$   
286 are nonnegative). For our purposes, we conclude that the spread in spawning age  
287 has very little impact on the model dynamics (too slight to justify an illustration,  
288 in fact), and so our models do not indicate that it is an important difference  
289 between chinook and coho population dynamics.

#### 290 4.2. Mechanism of environmental forcing

291 To illustrate the difference between population responses to different mech-  
292 anisms of environmental forcing we compare the cases with (1) variability in  
293 survival in each ocean year, (2) variability in survival at the age of ocean entry  
294 only and (3) variability in the spawning age distribution. Random variabil-  
295 ity in survival appears to preferentially excite the geometrically decaying mode,  
296 while variability in the spawning age preferentially excites the cyclic mode. This  
297 conclusion holds for all five of our model cases: the resonant frequency is about  
298  $0.33 \text{ yr}^{-1}$  for the coho salmon, whose dominant age of spawning is three years,

299 and about  $0.25 \text{ yr}^{-1}$  for the chinook salmon, whose dominant age of spawning is  
300 four years (not shown here, see next example). The one exception is that for the  
301 chinook model with  $s^\circ = 0.28 \text{ yr}^{-1}$ , there is a strong low-frequency component  
302 with variation in spawning age as well as the period-4 component.

303 We illustrate this general result with the case for coho salmon with  $s^\circ =$   
304  $0.28 \text{ yr}^{-1}$  by comparing the frequency responses to survival varying at all ages,  
305 for survival varying only at age 1, the presumed age of ocean entry, and for vari-  
306 ability in spawning age, then presenting examples of time series for each case.  
307 Both frequency responses to environmental variability in survival (Fig. 4a) de-  
308 cline from very low frequency, leveling off slightly at a frequency just below that  
309 corresponding to period 3 (the dominant age of spawning for coho salmon), then  
310 decline for higher frequency. The simulations indicate up to approximately 20  
311 percent greater variability than the analytical model in both survival cases. The  
312 case with variable ocean survival at all ages (Fig. 4b) is skewed more toward  
313 variability at low frequencies. The frequency response to environmental variabil-  
314 ity in the spawning age distribution increases from low frequency to a resonance  
315 at a frequency slightly greater than that corresponding to period three, the  
316 dominant age of spawning, consistent with cohort resonance.

317 The time series for each case (Fig. 5) indicate a visually discernable differ-  
318 ence between populations driven by environmental variability in survival and  
319 environmental variability in spawning age distribution. The population with  
320 environmental forcing of spawning age (Fig. 5c) has clear indications of cohort  
321 resonant behavior near period 2 yr to 4 yr, while the populations with environ-  
322 mental forcing of survival tend toward 5-10 yr fluctuations with little variability.  
323 The difference in the magnitude of variability between the series with varying  
324 survival is as expected from the difference in area under the two thin lines in  
325 Fig. 4a.

### 326 *4.3. Population observation*

327 To determine the effects of the type of observation on the time scales of  
328 variability we compared the results of observing recruitment to the results of

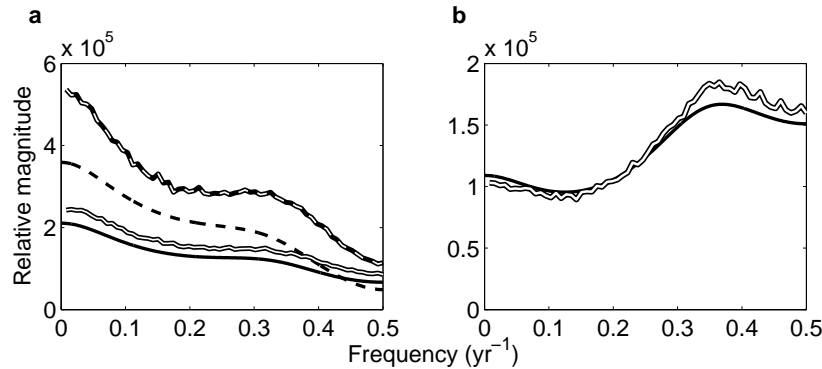


Figure 4: Magnitude of frequency response of recruitment for the linearized model (thin lines) and nonlinear simulations (bordered lines) for environmental forcing of (a) early ocean survival rate (solid lines) and ocean survival at all ages (dashed lines), and (b) spawning age distribution for coho salmon with  $s^\circ = 0.28 \text{ yr}^{-1}$ . See the Appendix (equation A.10) for derivation of the linearized frequency response. Nonlinear frequency response curves are estimated by calculating the average magnitude (the square root of mean power at each frequency) of the fast Fourier transforms of 1000 simulation time series of length 128, and scaling the result by  $\sqrt{128} \sigma_E$ , to obtain the same units as the analytically-derived transfer function.

329 observing total abundance for each case. Generally, they all exhibited rela-  
 330 tively more 2-to-5-year oscillation in the recruitment and more low-frequency  
 331 fluctuation in the total abundance.

332 To illustrate the difference between different types of population observa-  
 333 tions, we show the results of observing recruitment with the results of observing  
 334 total abundance, for chinook salmon with typical survival ( $s = 0.85 \text{ yr}^{-1}$ ) and  
 335 environmental variability in the spawning age distribution (Fig. 6). The spec-  
 336 tral response of recruitment increases from low frequency to a peak at about  
 337  $0.25 \text{ yr}^{-1}$ , the frequency expected for chinook salmon with dominant age of  
 338 reproduction at 4 yr, then declines. The spectral response of total abundance,  
 339 the sum of several cohorts, declines monotonically from low frequency, showing  
 340 only a hint of the resonance present in recruitment.

341 The time series of these two cases (Fig. 7) reflect these characteristics. The  
 342 time series from the population with observations of recruitment of a chinook  
 343 salmon population with environmental forcing of spawning age appears to have  
 344 a preponderance of variability on time scales of 2 yr to 5 yr, while the time

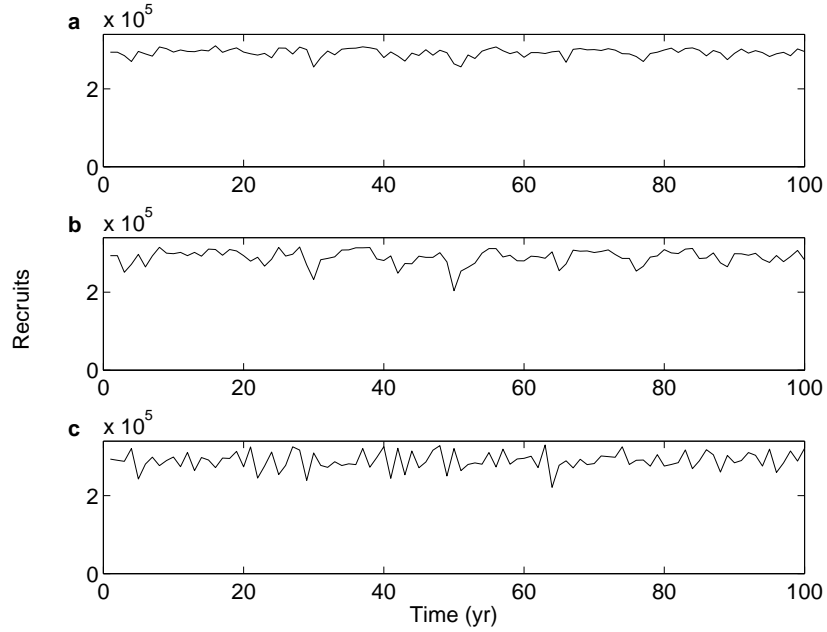


Figure 5: Time series of recruitment in simulations with environmental forcing of (a) early ocean survival ( $\sigma_E = 0.085$ ), (b) ocean survival at all ages ( $\sigma_E = 0.085$ ), and (c) spawning age distribution ( $\sigma_E = 0.2$ ) for coho with  $s^\circ = 0.28 \text{ yr}^{-1}$ . Identical sequences of standard normal random variables were used as the forcing signal in order to allow a comparison of filtering by different demographic mechanisms.

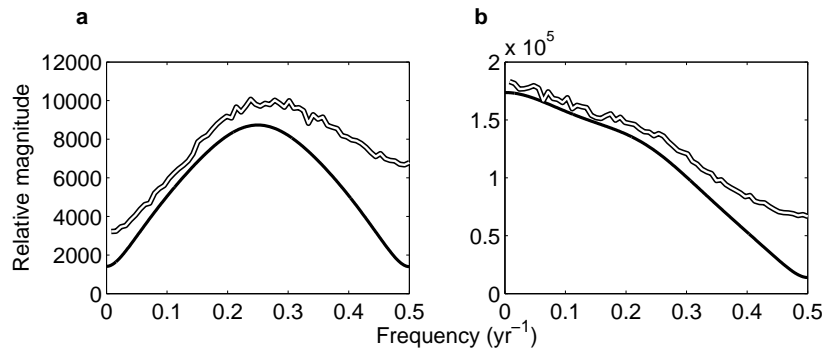


Figure 6: Magnitude of frequency response of (a) recruitment and (b) total abundance for the linearized model (black line) and nonlinear simulations (bordered line; 1000 simulations of length 128) for environmental forcing of spawning age distribution for chinook salmon with  $s = 0.85 \text{ yr}^{-1}$ .

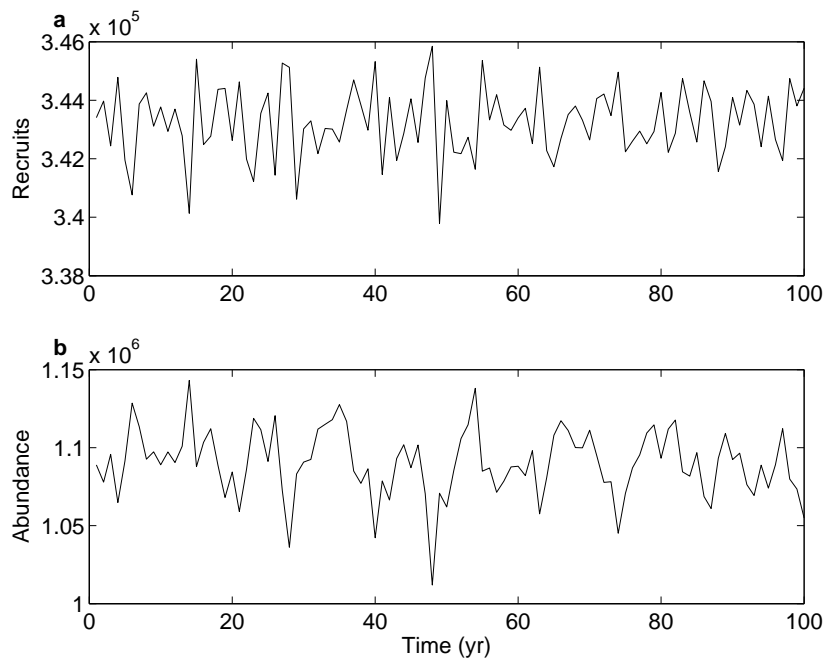


Figure 7: Time series of (a) recruitment and (b) total abundance from a single simulation with environmental forcing of spawning age distribution ( $\sigma_E = 0.2$ ) for chinook salmon with  $s = 0.85 \text{ yr}^{-1}$ .

345 series from the observation of abundance appears to be a smoothed version of  
 346 that.

#### 347 4.4. Long-term mean survival

348 To illustrate the differences between populations operating at different levels  
 349 of long-term survival we compared the coho salmon recruitment from a model  
 350 with environmental variability in spawning age distribution with each of the  
 351 three survival levels, typical, small and very small (Fig. 8). The shift to lower  
 352 constant survivals could result from fishing or a shift in climate. The frequency  
 353 responses with these three survivals have similar shapes but differ substantially  
 354 in scale. The resonance at period just less than 3 years is dominant because  
 355 the variability is in spawning age distribution. Note the greater increase in  
 356 sensitivity to low frequencies as the survival decreases to its lowest level.

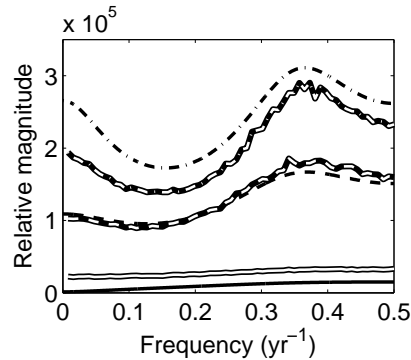


Figure 8: Magnitude of frequency response of recruitment for the linearized model (thin lines) and nonlinear simulations (bordered lines; 1000 simulations of length 128 with  $\sigma_E = 0.2$ ) for environmental forcing of spawning age distribution for coho with  $s = 0.85 \text{ yr}^{-1}$  (solid lines),  $0.28 \text{ yr}^{-1}$  (dashed lines), and  $0.2 \text{ yr}^{-1}$  (dash-dot lines).

357 The time series of these three cases (Fig. 9) appear to have similar frequency  
 358 content, but different levels of variability as expected from Fig. 8. Importantly,  
 359 they also underscore the fact that as survival declines variability increases as in  
 360 Fig. 8, as the equilibrium recruitment declines.

## 361 5. Discussion

362 These analyses provide an understanding of how various population charac-  
 363 teristics shape the response of salmon populations to environmental variability  
 364 on various time scales. Salmon population variability does not simply follow  
 365 variability in the environment as is commonly assumed, but rather the observed  
 366 response is shaped by three factors: (a) the life history point of impact of  
 367 the environment, (b) how the population is censused, and (c) pre-conditioning  
 368 by long-term changes in survival. These considerations have important conse-  
 369 quences for the management of salmon populations and the anticipation of the  
 370 effects of large-scale environmental change. The dynamics of salmon responses  
 371 to the environment are, of course, not unique, but rather are closely related to  
 372 those of other higher trophic level, age-structured species (McCann et al., 2003;  
 373 Bjørnstad et al., 2004).

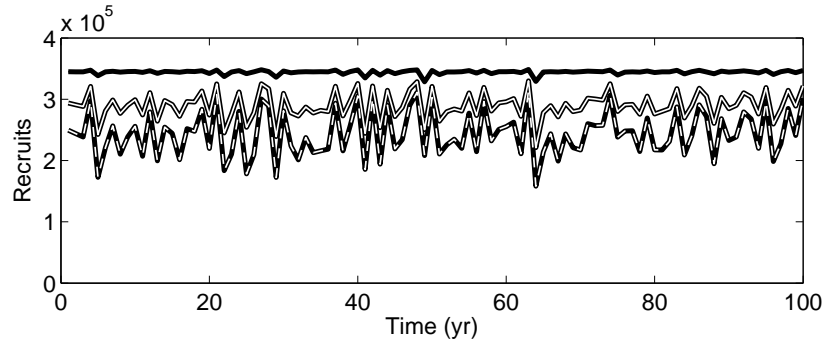


Figure 9: Time series of recruitment in simulations with environmental forcing of spawning age distribution ( $\sigma_E = 0.2$ ) for coho with  $s = 0.85 \text{ yr}^{-1}$  (solid black),  $0.28 \text{ yr}^{-1}$  (white with black border), and  $0.2 \text{ yr}^{-1}$  (dashed white on black). Identical sequences of standard normal random variables were used as the forcing signal in order to allow a comparison of filtering at different survival rates.

374 The importance of cohort resonance to climate change is enhanced by the  
375 finding that its effects intensify with decreasing survival. There is concern over  
376 the effects of climate change on fisheries, and how management should change to  
377 mitigate those changes (*e.g.*, Perry et al., 2010). The basic resonance mode with  
378 period  $T$  appears as the second and third eigenvalues in the linearized model, a  
379 conjugate pair. It is well known in linear age-structured models, as the echo ef-  
380 fect (Sykes, 1969; Caswell, 2001), and was identified earlier as a potential cause  
381 of observed cycles in some salmon populations (Myers et al., 1998). However,  
382 increasing cohort resonance with fishing has not been mentioned as a factor in  
383 the variability in fished populations. Knowing that high levels of fishing and  
384 specific time scales of environmental variability can increase overall population  
385 variability will be valuable in formulating management policies to maintain sus-  
386 tainability. The additional variability increases the risk of population collapse  
387 in addition to that risk incurred by reducing mean abundance. In addition,  
388 knowing that fish populations could be more sensitive to some time scales than  
389 others will aid in the explanation of changes in fisheries' variability if the time  
390 scales of forcing change with climate. Potential intensification of cohort reso-  
391 nance through increased fishing also underscores the importance of Bjørnstad's

392 (2004) warning regarding the low-frequency effect of cohort resonance, sensi-  
393 tivity to very low-frequency environmental variability. Fishing increases the  
394 chances that populations, even when driven by white noise in the environment,  
395 could generate very slowly changing signals that could be mistaken for the ef-  
396 fect of a slowly changing climate. This hard-to-detect long-timescale change  
397 may present a third increase in threat when coupled with reduced abundance  
398 and increased variability due to fishing. Note that this increased sensitivity at  
399 low frequencies was seen in coho salmon (Fig. 8) and also in chinook salmon  
400 with  $s = 0.28 \text{ yr}^{-1}$  (as noted at the end of section 4.2).

401 Differences in the dynamic responses of populations to temporal variability  
402 at different points in the species's life history are not commonly considered. For  
403 salmon (and most other marine fish), while the effects of variability in survival  
404 are widely appreciated, the authors are unaware of any description of the ef-  
405 fects of variability in spawning age distribution on population dynamics, such  
406 as on cohort resonance. Here we found that the different mechanisms involving  
407 variability in survival and variability in spawning age distribution preferentially  
408 excited different fundamental modes of variability; hence these differences are  
409 clearly important. In addition to variability in spawning age exciting a com-  
410 pletely different mode than variability in survival, responses to varying survival  
411 at ocean entry and varying total survival also differed, with less sensitivity to  
412 low frequencies resulting from variability in early ocean survival than from vari-  
413 ability in total survival. This further motivates efforts to discover the ages and  
414 locations at which variability in salmon marine survival occurs. This may be  
415 related to the difference in population persistence between these two survival  
416 mechanisms in earlier analysis (Botsford et al., 2005), where population variabil-  
417 ity was greater when it occurred at the age of return to the river for spawning,  
418 rather than the age of ocean entry of smolts. In that case this difference occurs  
419 because of the Law of Large Numbers, and the fact that the logarithm of the  
420 number of spawners is the sum of several random survivals when variability is  
421 at the age of entry, but only one random survival when it is at the age of return.

422 In our models, varying age of spawning causes much more oscillation at the

423 period of the generation length and less low-frequency fluctuation than varying  
424 survival does. This might be because changes in central spawning age have a  
425 double effect on recruitment, removing fish from one year's stock of potential  
426 spawners and adding them to the next or previous year's potential spawning  
427 stock. This perturbation has a direct effect on two cohorts' recruitment, which  
428 is echoed in subsequent generations when those cohorts spawn. Fluctuations  
429 in survival, on the other hand, whether they affect one cohort or many, cannot  
430 have this double effect, with the likely consequence that the period- $T$  echo effect  
431 is not as extreme.

432 The difference in frequency content between a catch (or abundance) series  
433 and a recruitment series was known previously (*e.g.*, Botsford, 1986), but there  
434 has been renewed interest in it. That difference basically follows from the Law  
435 of Large Numbers and the fact that when recruitment is the source of temporal  
436 variability, abundance will have a lower coefficient of variation because it is the  
437 sum of several recruitments, and hence can be expected to be a smoothed version  
438 of the recruitment signal, *i.e.*, to emphasize lower frequencies. As the value of  
439 constant harvest rate increases, the number of cohorts summed diminishes, and  
440 hence higher frequencies are observed.

441 The major difference between the population dynamics of coho salmon and  
442 chinook salmon revealed here is that they would be most sensitive to different  
443 time scales of environmental variability, as determined by the difference between  
444 the dominant age of spawning in each. Also, one explanation proposed for the  
445 fact that coho salmon declined near 1980, while chinook salmon did not, was  
446 that narrower width of the coho spawning age distribution. The effect of width  
447 of the spawning age distribution we determined here was not strong enough  
448 to support this hypothesis, leaving open the possibility that coho salmon were  
449 merely following a decline in ocean survival which did not decline for chinook  
450 salmon. These theoretical results are not definitive regarding specific stocks;  
451 rather they provide a context for further detailed investigations of the hundreds  
452 of coho and chinook salmon populations along the west coast of the U.S.

453 As with other structured-population models (Nisbet and Gurney, 1982; Bjørnstad et al.,

2004; Greenman and Benton, 2003), this model’s response to environmental fluctuation is predicted well by the linearization at the deterministic model’s fixed point. Like Greenman and Benton, we find amplification of noise as parameters vary — in our case, environmental noise is amplified more by the population dynamics when survival is reduced. In our case, however, this amplification is not associated with a nearby bifurcation, only with eigenvalues moving closer to the unit circle, a more general phenomenon.

As discussed above, we also observe major differences in frequency responses among different kinds of environmental influences and between different population measurements. The analysis in our Appendix explains these differences in terms of different geometric relationships between the forcing vectors, the eigenspaces corresponding to the eigenvalues of the linearization, and the measurements. The projection of the forcing vectors  $\vec{H}$  into each dynamical subspace determines how strongly the environmental noise stimulates motion in that subsystem, and therefore how prominent resonance at that frequency is in the population dynamics. Similarly, different observations — total population and recruitment — include the different subsystems in different proportions, and so each mode of population behavior is more visible in some observations than others (see the Appendix for the mathematical treatment of these ideas). This analysis, together with the diversity in frequency responses we see in our models, points to the importance of understanding the relationship between the eigenspace structure of the linearization and the relative importances of the resonant frequencies associated with each eigenspace. As an analytical technique, this approach may be useful in multispecies ecological models as well as in structured population models.

The results obtained here provide the means both to begin to explain current differences in responses to the environment by the same species at different locations, and to project differences in future responses on the basis of projected changes in time scales of variability in the environment. Current differences in responses by populations of the same species are typically presumed to imply a difference in environmental forcing, but they may be due to differences in life

485 histories or differences in preconditioning because they are fished at different  
486 intensities. Future changes in time scales of variability are expected on the  
487 basis of paleological records (*e.g.*, past changes in the time scales of variability  
488 of El Niño events as observed in corals and other media, Jones et al., 2009) or  
489 predictions from global climate models (Timmermann et al., 1999).

#### 490 **Acknowledgments**

491 This research is part of the GLOBEC Northeast Pacific program and was  
492 funded by National Science Foundation grants NSF OCE0003254 and NSF  
493 OCE0815293. Any opinions, findings, and conclusions or recommendations ex-  
494 pressed in this material are those of the author(s) and do not necessarily reflect  
495 the views of the National Science Foundation.

496 Anderson, C., Hsieh, C., Sandin, S., Hewitt, R., Hollowed, A., Beddington,  
497 J., May, R., Sugihara, G., 2008. Why fishing magnifies fluctuations in fish  
498 abundance. *Nature* 452 (7189), 835–839.

499 Barrowman, N., Myers, R., Hilborn, R., Kehler, D., Field, C., 2003. The vari-  
500 ability among populations of coho salmon in the maximum reproductive rates  
501 and depensation. *Ecological Applications* 13, 784–793.

502 Bernstein, D., 1992. Some open problems in matrix theory, arising in linear  
503 systems and control. *Linear Algebra and its Applications* (162–164), 409–432.

504 Beverton, R., Holt, S., 1957. On the dynamics of exploited fish populations.  
505 *Fishery Investigations, Series II. Marine Fisheries*, Great Britain Ministry of  
506 Agriculture, Fisheries and Food 19, 533.

507 Bjørnstad, O. N., Fromentin, J. M., Stenseth, N., Gjøsæter, J., 1999. Cycles and  
508 trends in cod populations. *Proceedings of the National Academy of Sciences*  
509 USA 96, 5066–5071.

510 Bjørnstad, O. N., Nisbet, R. M., Fromentin, J. M., 2004. Trends and cohort  
511 resonant effects in age-structured populations. *Journal of Animal Ecology*  
512 73 (6), 1157–1167.

- 513 Botsford, L., 1986. Effects of environmental forcing on age-structured popula-  
514 tions: northern California Dungeness crab (*Cancer magister*) as an example.  
515 Canadian Journal of Fisheries and Aquatic Sciences 43 (11), 2345–2352.
- 516 Botsford, L., 1997. Dynamics of populations with density-dependent recruit-  
517 ment and age structure. In: Tuljapurkar, S., Caswell, H. (Eds.), Structured  
518 Population Models in Marine, Terrestrial, and Freshwater Systems. Chapman  
519 and Hall, New York, Ch. 12.
- 520 Botsford, L., Lawrence, C., Hill, M., 2005. Differences in dynamic response of  
521 california current salmon species to changes in ocean conditions. Deep-Sea  
522 Research II (52), 331–345.
- 523 Botsford, L., Lawrence, C. A., 2002. Patterns of co-variability among california  
524 current chinook salmon, coho salmon, dungeness crab, and physical oceanographic  
525 conditions. Progress in Oceanography 53, 283–305.
- 526 Bradford, M., 1995. Comparative review of Pacific salmon survival rates. Canadian  
527 Journal of Fisheries and Aquatic Sciences 52, 1327–1338.
- 528 Caswell, H., 2001. Matrix population models: construction, analysis, and inter-  
529 pretation. Sinauer, Sunderland, MA.
- 530 Coronado, C., Hilborn, R., 1998. Spatial and temporal factors affecting survival  
531 in coho salmon (*Oncorhynchus kisutch*) in the Pacific Northwest. Canadian  
532 Journal of Fisheries and Aquatic Sciences 55 (9), 2067–2077.
- 533 Day, T., Rowe, L., 2002. Developmental thresholds and the evolution of reaction  
534 norms for age and size at life history transitions. American Naturalist 159,  
535 338–350.
- 536 Doornik, D. M., Ford, M. J., Teel, D. J., 2002. Patterns of temporal genetic  
537 variation in coho salmon: estimates of the effective proportion of 2-year-olds  
538 in natural and hatchery populations. Transactions of the American Fisheries  
539 Society 131, 1007–1019.

- 540 Elaydi, S. N., 1999. An Introduction to Difference Equations, 2nd Edition. Un-  
541 dergraduate Texts in Mathematics. Springer, New York.
- 542 Greenman, J. V., Benton, T. G., 2003. The amplification of environmental noise  
543 in population models: causes and consequences. *The American Naturalist*  
544 161 (2), 225–239.
- 545 Greenman, J. V., Benton, T. G., 2005. The frequency spectrum of structured  
546 discrete time population models: its properties and their ecological implica-  
547 tions. *Oikos* 110, 369–389.
- 548 Healey, M., 1991. Life history of Chinook salmon (*Oncorhynchus tshawytscha*).  
549 In: Groot, C., Margolis, L. (Eds.), *Pacific Salmon Life Histories*. UBC Press,  
550 Vancouver, Canada, pp. 313–393, 564 pp.
- 551 Hill, M., Botsford, L., Hastings, A., 2003. The effects of spawning age distri-  
552 bution on salmon persistence in fluctuating environments. *Journal of Animal*  
553 *Ecology* 72, 732–744.
- 554 Hirsch, M. W., Smale, S., 1974. *Differential Equations, Dynamical Systems, and*  
555 *Linear Algebra*. Academic Press.
- 556 Hsieh, C., Reiss, C., Hunter, J., Beddington, J., May, R., Sugihara, G., 2006.  
557 Fishing elevates variability in the abundance of exploited species. *Nature*  
558 443 (7113), 859–862.
- 559 Jones, P., Briffa, K., Osborn, T., Lough, J., van Ommen, T., Vinther, B.,  
560 Luterbacher, J., Wahl, E., Zwiwers, F., Mann, M., Schmidt, G., Ammann, C.,  
561 Buckley, B., Cobb, K., Esper, J., Goosse, H., Graham, N., Jansen, E., Kiefer,  
562 T., Kull, C., Kuttel, M., Mosley-Thompson, E., Overpeck, J., Riedwyl, N.,  
563 Schulz, M., Tudhope, A., Villalba, R., Wanner, H., Wolff, E., Xoplaki, E.,  
564 2009. High-resolution palaeoclimatology of the last millennium: a review of  
565 current status and future prospects. *The Holocene* 19 (1), 3–49.
- 566 Logerwell, E., Mantua, N., Lawson, P., Francis, R., Agostini, V., 2003. Tracking  
567 environmental processes in the coastal zone for understanding and predicting

- 568 Oregon coho (*Oncorhynchus kisutch*) marine survival. Fisheries Oceanography  
569 12 (6), 554–568.
- 570 McCann, K., Botsford, L., Hastings, A., 2003. Differential response of marine  
571 populations to climate forcing. Canadian Journal of Fisheries and Aquatic  
572 Sciences 60 (8), 971–985.
- 573 Moloney, C. L., Botsford, L., Largier, J. L., 1994. Development, survival and  
574 timing of metamorphosis of planktonic larvae in a variable environment: the  
575 dungeness crab as an example. Marine Ecology Progress Series 113, 61–79.
- 576 Myers, R. A., Mertz, G., Bridson, J. M., Bradford, M. J., 1998. Simple dynamics  
577 underlie sockeye salmon (*Oncorhynchus nerka*) cycles. Canadian Journal of  
578 Fisheries and Aquatic Sciences 55, 2355–2364.
- 579 Nisbet, R. M., Gurney, W. S. C., 1982. Modelling Fluctuating Populations.  
580 Wiley, Chichester.
- 581 Perry, R. I., Cury, P., Brander, K., Jennings, S., Mllmann, C., Planque, B.,  
582 2010. Sensitivity of marine systems to climate and fishing: concepts, issues  
583 and management responses. Journal of Marine Systems 79, 427–435.
- 584 Pyper, B., Peterman, R., Lapointe, M., Walters, C., 1999. Patterns of covari-  
585 ation in length and age at maturity of British Columbia and Alaska sock-  
586 eye salmon (*Oncorhynchus nerka*) stocks. Canadian Journal of Fisheries and  
587 Aquatic Sciences 56, 1046–1057.
- 588 Ricker, W., 1954. Stock and Recruitment. Fisheries Research Board of Canada.
- 589 Sandercock, F., 1991. Life history of coho salmon (*Oncorhynchus kisutch*). In:  
590 Groot, C., Margolis, L. (Eds.), Pacific Salmon Life Histories. UBC Press,  
591 Vancouver, Canada, pp. 397–445, 564 pp.
- 592 Sissenwine, M. P., Shepherd, J. G., 1987. An alternative perspective on recruit-  
593 ment overfishing and biological reference points. Canadian Journal of Fisheries  
594 and Aquatic Sciences 44, 913–918.

- 595 Sykes, Z. M., 1969. On discrete stable population theory. *Biometrics* 25 (2),  
596 285–293.
- 597 Teo, S., Botsford, L., Hastings, A., 2009. Spatio-temporal covariability in coho  
598 salmon (*Oncorhynchus kisutch*) survival, from California to southeast Alaska.  
599 Deep-Sea Research Part II.
- 600 Timmermann, A., Oberhuber, J., Bacher, A., Esch, M., Latif, M., Roeckner,  
601 E., 1999. Increased El Niño frequency in a climate model forced by future  
602 greenhouse warming. *Nature* 398, 694–697.
- 603 Vollestad, L., Peterson, J., Quinn, T., 2004. Effects of freshwater and marine  
604 growth rates on early maturity in male coho and chinook salmon. *Transactions*  
605 *of the American Fisheries Society* 133, 495–503.
- 606 Young, K., 1999. Environmental correlates of male life history variation coho  
607 salmon populations from two Oregon coastal basins. *Transactions of the*  
608 *American Fisheries Society* 128, 1–16.

609 **Appendix A. General Mathematical Results**

610 The linearization of a stochastic map

$$\vec{x}(t) = F(\vec{x}(t-1), \xi(t), \xi(t-1), \dots, \xi(t-L)), \quad \vec{x}(t) \in \mathbb{R}^n, \quad \xi(t) \in \mathbb{R}, \quad (\text{A.1})$$

611 where (without loss of generality)  $\mathbb{E}(\xi(t)) = 0$ , is

$$\vec{y}(t) \approx \mathbf{J}\vec{y}(t-1) + \sum_{l=0}^L \vec{H}(l)\xi(t-l) \quad (\text{A.2})$$

612 where  $\vec{x}(t) = \tilde{\vec{x}} + \vec{y}(t)$ ,  $\tilde{\vec{x}}$  is a fixed point of  $F(\vec{x}, 0)$ ,  $\mathbf{J} = \left( \frac{\partial F_i}{\partial x_j} \right) |_{(\tilde{\vec{x}}, 0)}$  is the  
 613 Jacobian matrix of  $F$  at  $\vec{x} = \tilde{\vec{x}}$  and  $\xi = 0$ ,  $\vec{H}(l) = \frac{\partial F}{\partial \xi(t-l)}(\tilde{\vec{x}}, 0)$  is a vector  
 614 expressing the dependence of  $F$  on the noise terms, and  $L$  is the maximum  
 615 time lag at which stochastic perturbations affect  $F$  directly. Let  $\vec{v}_i$  and  $\vec{u}_i$  be  
 616 the left and right eigenvectors of  $\mathbf{J}$ , respectively, and  $\lambda_i$  its eigenvalues, so that  
 617  $\vec{v}_i \mathbf{J} = \lambda_i \vec{v}_i$  and  $\mathbf{J} \vec{u}_i = \lambda_i \vec{u}_i$ . In this paper we only consider matrices that have  
 618 all distinct eigenvalues.

619 We change to the natural coordinate system of  $\mathbf{J}$ : Let

$$\mathbf{U} = (\vec{u}_1, \dots, \vec{u}_n), \quad \mathbf{V} = \begin{pmatrix} \vec{v}_1 \\ \vdots \\ \vec{v}_n \end{pmatrix}, \quad \mathbf{\Lambda} = \begin{pmatrix} \lambda_1 & 0 & \cdots & 0 \\ 0 & & & \\ \vdots & \ddots & & \vdots \\ 0 & \cdots & 0 & \lambda_n \end{pmatrix}, \quad (\text{A.3})$$

620 with  $\mathbf{J} = \mathbf{U}\mathbf{\Lambda}\mathbf{V} = \sum_i \lambda_i \vec{u}_i \vec{v}_i$  and  $\mathbf{U}\mathbf{V} = \mathbf{V}\mathbf{U} = \mathbf{I}$ . Then for  $\vec{w} = \mathbf{V}\vec{y}$ ,

$$\begin{aligned} \vec{w}(t) = \mathbf{V}\vec{y}(t) &= \mathbf{\Lambda}\mathbf{V}\vec{y}(t-1) + \sum_{l=0}^L \vec{G}(l)\xi(t-l) \\ &= \mathbf{\Lambda}\vec{w}(t-1) + \sum_{l=0}^L \vec{G}(l)\xi(t-l) \end{aligned} \quad (\text{A.4})$$

621 with  $\vec{G}(l) = \mathbf{V}\vec{H}(l)$ . Using the terms of this transformed vector  $\vec{w}$ , the vector  
 622 of deviations from equilibrium can be written as a sum of eigenvectors,  $\vec{y} =$   
 623  $\sum_i w_i \vec{u}_i$ . Since  $\mathbf{\Lambda}$  is diagonal, the dynamics of each  $w_i(t)$  is uncoupled from the

624 others:

$$w_i(t) = \lambda_i w_i(t-1) + \sum_{l=0}^L g_i(l) \xi(t-l) \quad (\text{A.5})$$

625 where  $g_i(l) = \vec{v}_i \vec{H}(l)$  is the  $i$ th entry of  $\vec{G}(l)$ . Thus,  $\vec{w}(t)$  is the state of the  
 626 linear system decomposed into its independent subsystems, and the vectors  
 627  $\vec{G}(l)$  represent the stochastic forcing resolved into the decomposed coordinate  
 628 system.

629 *Forcing and measurement*

630 The entries of the transformed vector  $\vec{G}$  reveal how strongly the environmen-  
 631 tal forcing acts on each subsystem of the linearized system. Different kinds of  
 632 forcing (i.e. survival, age of maturation) are distributed differently among the  
 633 different subsystems, characterized by the projection of the forcing into each  
 634 eigenspace,  $g_i(l) = \vec{v}_i \vec{H}(l)$  for each  $i$  and  $l$ . If  $g_i(l) = 0$  for all  $l$ , there is no  
 635 fluctuation in the subspace containing eigenvector  $\vec{u}_i$ , that is, no fluctuation in  
 636  $w_i$ . In general, the more  $\vec{H}$  is aligned with certain eigenvectors  $\vec{u}_i$ , the more the  
 637 fluctuations caused by the forcing signal will be concentrated in those subsys-  
 638 tems.

639 Similarly, a particular measurement generally observes some subsystems  
 640 more than others. Assume we are observing the population via a scalar mea-  
 641 surement, whether annual total population, recruitment or catch, represented  
 642 as  $M(t) = Q(\vec{x}(t))$ . Let us assume that  $Q(\vec{x})$  is differentiable at the fixed point  
 643  $\tilde{\vec{x}}$ . In the weak-noise limit this quantity also can be described by a linear ap-  
 644 proximation,

$$\begin{aligned} Q(\vec{x}(t)) &= Q(\tilde{\vec{x}}) + \sum_i \frac{\partial Q}{\partial x_i}(\tilde{\vec{x}}) y_i(t) + \text{O}(|y|^2) \\ &= Q(\tilde{\vec{x}}) + \sum_i q_i y_i(t) + \text{O}(|y|^2). \end{aligned} \quad (\text{A.6})$$

645 The measurement  $M(t)$  is approximated by the linear quantity  $Q(\tilde{\vec{x}}) + \sum_i q_i y_i(t)$ ,  
 646 which differs by only a constant from  $\sum_i q_i x_i(t)$ , and fluctuation in either quan-  
 647 tity has the same characteristics as fluctuation in  $\sum_i q_i y_i(t)$ . We can repre-  
 648 sent the linearized measurement as a vector product  $\vec{q} \vec{y}(t)$ , using a row vector

649  $\vec{q} = (q_1, \dots, q_n)$ . Changing to the natural coordinates of  $\mathbf{J}$ ,

$$\vec{q}\vec{y}(t) = \vec{q} \sum_i w_i(t) \vec{u}_i = \sum_i \vec{q}\vec{u}_i w_i(t) = \sum_i m_i w_i(t). \quad (\text{A.7})$$

650 Then  $m_i = \vec{q}\vec{u}_i$  expresses how strongly the motion in the subsystem containing  
651  $w_i$  is reflected in the measurement.

652 *Frequency Analysis*

653 For the frequency analysis, take  $\vec{w}(t) = \vec{0}$  and  $\xi(t) = 0$  for all  $t < 0$ . Then  
654 we may write the  $Z$ -transform (Elaydi, 1999):

$$\begin{aligned} \hat{w}(z) &\equiv \sum_{k=0}^{\infty} \vec{w}(k) z^{-k} \\ &= \sum_{k=0}^{\infty} \left( \mathbf{\Lambda} \vec{w}(k-1) + \sum_{l=0}^L \vec{G}(l) \xi(k-l) \right) z^{-k} \\ &= \mathbf{\Lambda} \underbrace{\sum_{k=0}^{\infty} \vec{w}(k-1) z^{-k}} + \sum_{l=0}^L \vec{G}(l) \underbrace{\sum_{k=0}^{\infty} \xi(k-l) z^{-k}}. \end{aligned} \quad (\text{A.8})$$

655 The bracketed expressions are themselves  $Z$ -transforms of shifted sequences of  
656  $\vec{w}$  and  $\xi$ , so that by the shift property of the  $Z$ -transform (Elaydi, 1999),

$$\hat{w}(z) = \mathbf{\Lambda} z^{-1} \hat{w}(z) + \sum_{l=0}^L \vec{G}(l) z^{-l} \hat{\xi}(z) \quad (\text{A.9})$$

657 or

$$\hat{w}(z) = (1 - \mathbf{\Lambda} z^{-1})^{-1} \sum_{l=0}^L \vec{G}(l) z^{-l} \hat{\xi}(z). \quad (\text{A.10})$$

658  $(1 - \mathbf{\Lambda} z^{-1})^{-1}$  is a diagonal matrix with entries  $\frac{1}{1 - \lambda_i z^{-1}} = \frac{z}{z - \lambda_i}$ . Consequently  
659 the  $Z$ -transformed deviation vector,

$$\hat{y}(z) = \mathbf{U} \hat{w}(z) = \sum_{i=1}^n \left( \vec{u}_i \frac{z}{z - \lambda_i} \sum_{l=0}^L g_i(l) z^{-l} \hat{\xi}(z) \right), \quad (\text{A.11})$$

660 is a linear sum of rational functions of  $z$ , with peaks tending to be near the  
661 eigenvalues of  $\mathbf{J}$ .

662 Similarly, in the frequency analysis of a measurement  $M(t)$ ,

$$\begin{aligned}
\hat{M}(z) &= \sum_{k=0}^{\infty} M(k) z^{-k} \\
&\approx \sum_k (Q(\tilde{x}) + \sum_i m_i w_i(k)) z^{-k} \\
&= \sum_k Q(\tilde{x}) z^{-k} + \sum_i m_i \hat{w}(z).
\end{aligned}
\tag{A.12}$$

663 It is appropriate to discard the constant part of  $M(t)$  since we are concerned  
664 with year to year variation:

$$\begin{aligned}
\sum_i m_i \hat{w}(z) &= \sum_i \left[ m_i \sum_{l=0}^L g_i(l) \frac{z}{z - \lambda_i} z^{-l} \hat{\xi}(z) \right] \\
&= T_M(z) \hat{\xi}(z).
\end{aligned}
\tag{A.13}$$

665 The frequency response  $T_M(z)$  of the measurement  $M(t)$  is a weighted sum of  
666 the frequency responses for each subsystem,  $T_i(z) = \frac{z}{z - \lambda_i}$ , each weighted both  
667 by the strength of environmental forcing in that subsystem at each lag,  $g_i(l)$ ,  
668 and by the “emphasis” of the subsystem in the measurement,  $m_i$ .